

IMECE2015-52103

THEORETICAL RANGE AND TRAJECTORY OF A WATER JET

Ben Trettel*

Department of Mechanical Engineering
 University of Texas at Austin
 Austin, TX 78712
 Email: ben.trettel@gmail.com

Ofodike A. Ezekoye

Department of Mechanical Engineering
 The University of Texas at Austin
 Austin, TX 78712
 Email: dezekoye@mail.utexas.edu

ABSTRACT

The trajectory of a water jet is important in many applications, including fire protection, irrigation, and decorative fountains. Increasing the maximum distance the jet travels by changing the nozzle or other variables is often desirable. This distance could be the horizontal range (also often called the reach or throw) or the maximum vertical height. Which factors control the trajectory are unclear. Consequently, a simple analytical model is developed which provides a qualitative understanding of the system. This model differs significantly from previous models. Previous models either used a dragless trajectory, which is correct according to potential flow theory if the jet does not break into droplets, or treated the trajectory as if droplets formed immediately upon leaving the nozzle. Both approaches have been noted to be unsatisfactory by past researchers. Our model compares favorably against available experimental data. Using our model, we show that the range decreases as the nozzle Froude number increases and that range increases as breakup length and droplet size increase.

NOMENCLATURE

0 conditions at nozzle exit
 b conditions at (time-averaged) breakup location
 g gas fluid type (air)
 l liquid fluid type (water)
 ρ_i fluid i mass density
 $\eta_h \equiv h/H$ jet height efficiency
 $\eta_R \equiv R/R_{\max, h_0=0}$ range efficiency

μ_i fluid i dynamic viscosity
 σ surface tension of water (marked l) immersed in atmospheric air (marked g)
 θ_i angle of motion of a particle in the 2D plane at location i (e.g., θ_0 is the firing angle)
 A_D droplet projected area ($= \pi D^2/4$ for spherical droplets)
 $Bo_{ij} \equiv (\rho_i g L_j^2)/\sigma$ Bond number of fluid i and length j ($Bo_{ij} \equiv We_{ij}/Fr_j$)
 C_d drag coefficient
 C_d^* reduced drag coefficient that accounts for the density ratio, Froude number, and droplet size
 d nozzle exit diameter
 D droplet diameter
 $D^* \equiv D/d$ droplet diameter normalized by the nozzle diameter (d)
 $Fr_j \equiv V_0^2/(g L_j)$ Froude number of length j
 L_b time-averaged breakup length of a liquid jet
 $L^* \equiv L_b/d$ breakup length normalized by nozzle diameter (d)
 g gravitational acceleration
 h maximum height obtained by a vertical fountain
 h_0 starting firing height
 $H \equiv V_0^2/(2g)$ theoretical maximum height (without drag or breakup) that can be obtained by a vertical fountain
 m_D droplet mass ($= \pi \rho_l D^3/6$ for spherical droplets)
 R horizontal range
 $R_{\max, h_0=0} \equiv V_0^2/g$ theoretical maximum horizontal range (without drag or breakup) that can be obtained by a trajectory with a no starting height ($h_0 = 0$)
 $Re_{ij} \equiv \rho_i L_j V_0/\mu_i$ Reynolds number of fluid i and length j

*Address all correspondence to this author.

$We_{ij} \equiv \rho_i L_j V_0^2 / \sigma$ Weber number of fluid i and length j
 V_i velocity at location i

1 INTRODUCTION

Water jets appear in fire protection as fire hose streams, in agriculture as irrigation sprinklers, and in architecture as decorative fountains. Despite the ubiquitous applications, the trajectory of a water jet is poorly understood. Typically, accurate predictions of the trajectory of a water jet require either empirical tables, charts, or correlations [1, 2, 3]. This empirical data applies only for particular water jet systems, and it may not generalize to other systems. Further, how specific features of water jet systems affect the trajectory is not particularly clear. Given those issues, two related problems are of interest. The first is the theoretical prediction of the height of a water jet shot vertically, for example, a fountain, or a water jet used to fight a high rise fire. The second is the theoretical prediction of the horizontal range of a water jet shot at a target from a distance, as is the typical case in a fire. Height and range here refer to the maximum extent of the trajectory.

The typical dynamics of these jets is as follows. Water is forced through a nozzle by a pressure differential. The flow becomes a free jet, after which it generally begins to break apart into droplets of various sizes. We define the coherent portion as the part of the jet which has not broken into droplets. The breakup process is unsteady, and consequently the coherent length of the jet varies in time. The phrase “breakup length” generally refers to the time average of length of the coherent portion of the jet. Generally, the breakup length and droplet sizes are functions of the water jet system including the nozzle geometry, turbulence, flow unsteadiness, and presence of air bubbles in the water, among other factors. For details on the breakup of liquid jets the reader is referred to Lin and Reitz [4] and Birouk and Lekic [5]. It is commonly hypothesized that decreasing spray formation (i.e., increasing the breakup length) increases the range [6, 7]. Theobald’s experiments [1] support this hypothesis, but there is no clear theoretical support. One major goal of this work is to demonstrate how different spray characteristics affect the trajectory to design systems with longer range and more favorable water distributions at the target.

There is a large body of research into water jet trajectory owing to the wide variety of applications. Much of this research is somewhat obscure, as researchers in fire protection tend to be unaware of research done by agricultural engineers, and vice versa. For brevity, only representative research can be cited. Also, as the initial coherent portion presents the challenge in this problem, research which focused on nozzles which atomized the water (such as fire fighting fog nozzles) are not part of the scope of this article. And while wind can provide a cross flow in the applications of interest, wind is neglected in this work for simplicity. There are a large number of studies examining liquid

jet trajectory in crossflow, typically for gas turbine applications, and these may prove useful if this work is extended to include the effects of wind.

Conducting water jet trajectory experiments in a truly quiescent atmosphere is difficult. Almost all tests were conducted outdoors owing to the long range of these jets. Outdoor tests include those by Freeman [8], Rouse, Howe, and Metzler [6], and Arato, Crow, and Miller [9]. Testing indoors would eliminate the possibility of interference from wind. Theobald’s tests are the only we are aware of that were done entirely indoors. Past tests also tended not to describe important details. Few have discussed the nozzle exit velocity profile aside from Arato, Crow, and Miller [9], Freeman [8], and Theobald [1], and the latter did so only qualitatively. The nozzle exit velocity profile is known to strongly influence the breakup process [5, 10]. Arato, Crow, and Miller [9] also were the only to report the turbulence intensity, which Rouse, Howe, and Metzler [6] indicates is of fundamental importance to the jet breakup and trajectory. The reduction of breakup length as turbulence intensity increases was shown by Ervine and Falvey [11], but we are not aware of studies which looked at the effect of varying turbulence intensity on the trajectory. More careful tests characterizing these effects on the trajectory are overdue. Unfortunately, the possibility of reducing the space needed for indoor tests with scale modeling is limited because surface tension does not vary adequately between fluids or through adding a surfactant.

Most previous theoretical work on this subject either neglected the effect of drag on the trajectory [6, 12], or treated the trajectory as if it consisted of droplets for its entire duration [13], as is the case for an atomized spray. Some of the latter studies used linear drag models to simplify analysis relative to a quadratic drag law [14]. None of these approaches are particularly accurate. In order to match experimental data, Hatton and Osborne [15] and Hatton, Leech, and Osborne [16] use an empirical drag law with a variable power on the velocity, which has no theoretical justification. This model cannot show the effect of changing the droplet size distribution or breakup length, and the model can be considered a complicated curve fit to a particular water jet system. This highlights an additional shortcoming of past models. Past models do not use explicitly use the breakup characteristics of a nozzle, resulting in two related issues: 1. inaccuracy from either neglecting drag altogether or applying an inappropriate drag model and/or 2. the failure of the model to generalize to water jet systems with different breakup characteristics.

A model which shares some similarities with ours was developed by Murzabaeb and Yarin [17]. They characterize the fit between the data and their model as satisfactory. The authors used correlations for breakup length and droplet size as the initial conditions for a numerical turbulent multiphase boundary layer calculation, from which they obtained the trajectory of the water jet. Their model included the computation of air entrainment, and it is quite complex when compared against ours.

Isaev [18] showed theoretically that the trajectory in the dragless case depends on $Fr_d \equiv V_0^2/(gd)$, where V_0 is the spatially averaged velocity of the water jet emerging from the nozzle, and d is the diameter of the nozzle. Using an analogy with pipe flow, Isaev [18] developed an expression for the range with drag which also included Fr_d . Arato, Crow, and Miller [9] conducted vertical height experiments and noticed that jet height efficiency ($\eta_h \equiv h/H$), defined as the jet height (h) divided by the maximum height that a jet could obtain without drag (H), was a function of Fr_d . They also developed a correlation for η_h as a function of Fr_d , for which η_h would have exceeded 1 if Fr_d were small enough, an impossibility. Arato, Crow, and Miller [9] provided very little explanation to justify the use of Fr_d . Hatton and Osborne [15] suggested that if their model had quadratic drag, then the Froude number is the important parameter. Their model used a nonphysical drag parameter which they called k . If $k \equiv \frac{3}{4}(\rho_g/\rho_l)C_d/D$ then their quadratic drag model corresponds exactly to a model of the real trajectory of a spherical particle of diameter D . The representative droplet diameter D is roughly proportional to d , the nozzle diameter. Assuming this proportionality holds, a Froude number (Fr_d) can be constructed in their exact solution. Hatton and Osborne [15] also noted that “ k becomes zero at $Fr_d = 37$ and would be negative for values of Fr_d below 37. This, of course is not possible, and [the proposed model] was arranged to put k at the small value of 0.001 for $Fr_d < 37$ ”.

Tuck [19] demonstrated that the lead order terms of the potential flow solution for a water jet’s trajectory (i.e., a trajectory with no breakup) are identical to the trajectory of a dragless projectile without wind. Further, Oehler [20, 21] showed experimentally that under conditions in which no breakup occurs, the trajectory of a water jet launched at an angle is parabolic, consistent with a dragless trajectory. These observations were further confirmed by Kawakami [22], who observed that the range of a water jet equaled that of a dragless trajectory when the velocity was low enough.

These results indicate that the nozzle Froude number largely controls the maximum extent of the jet, and that there exists a critical Froude number, below which the jet experiences negligible drag in the absence of wind. Theoretical analysis of this situation as detailed in this paper indicates the Froude number is paramount in the trajectory problem. This analysis also shows that below a critical Froude number the jet does not appreciably break into droplets, and thus the range or height it attains is the maximum possible.

2 VERTICAL HEIGHT ANALYSIS

Theory. The vertical fountain case without wind is analyzed here. The jet is assumed to remain coherent and dragless until its height equals the breakup distance (L_b), after which the jet immediately breaks into spherical droplets of uniform diameter D . These droplets do not interact (i.e., they can overlap without any

collisions or other effects) and they do not change diameter (i.e., evaporation, coalescence, and secondary breakup are neglected). Further, the gas phase velocity is zero, meaning that there is no air entrainment.

For $x < L_b$, where x is the height above the nozzle, the equation of motion of the jet is

$$\ddot{x} = -g. \quad (1)$$

The same equation is used to find the maximum possible height without drag (H). If a jet is launched vertically at velocity V_0 , then $H = V_0^2/(2g)$. If the maximum height the water jet reaches is less than the breakup distance, then the jet never breaks up and equation 1 describes the entire trajectory.

The solutions to equation 1 are $\dot{x}(t) = V_0 - gt$ and $x(t) = V_0t - \frac{1}{2}gt^2$. These can be solved when $x = L_b$ to find that $\dot{x}(x = L_b) \equiv V_b = \sqrt{V_0^2 - 2gL_b}$. This result is used as the initial condition in the next stage of the trajectory.

Assuming that $L_b < H$, at $x = L_b$ the jet breaks into droplets of diameter D . The droplets are considered large enough for a quadratic drag law to apply (due to the high Reynolds number). Then the equation of motion for $x > L_b$ is

$$m_D\ddot{x} = -m_Dg - \frac{1}{2}\rho_g C_d A_D \dot{x}^2, \quad (2)$$

or assuming the droplets are spherical,

$$\frac{\pi}{6}\rho_l D^3 \ddot{x} = -\frac{\pi}{6}\rho_l D^3 g - \frac{1}{2}\rho_g C_d \frac{\pi}{4} D^2 \dot{x}^2. \quad (3)$$

After simplification, the equation of motion becomes

$$\ddot{x} = -g - \frac{3}{4} \frac{\rho_g}{\rho_l} \frac{C_d}{D} \dot{x}^2. \quad (4)$$

Then, through non-dimensionalization with $\tau \equiv t/(V_b/g)$ and $x^* \equiv x/(V_b^2/g)$ we find

$$\frac{d^2 x^*}{d\tau^2} = -1 - \underbrace{\frac{3}{4} \frac{\rho_g}{\rho_l} C_d \frac{V_b^2}{gD}}_{C_d^*} \left(\frac{dx^*}{d\tau} \right)^2. \quad (5)$$

If the coefficient on the final term is defined as C_d^* and $dx^*/d\tau$ is defined as v^* , then the equation is simplified:

$$\frac{dv^*}{d\tau} = - (1 + C_d^*(v^*)^2). \quad (6)$$

This equation can be integrated from time 0 (when the breakup starts and where $\dot{x} = V_b$) to find that

$$v^* = \frac{dx^*}{d\tau} = \frac{\tan \left[\text{atan} \left(\sqrt{C_d^*} \right) - \sqrt{C_d^*} \tau \right]}{\sqrt{C_d^*}}. \quad (7)$$

Integrating this equation from 0 to $\Delta h^* (\equiv (h - L_b)/H)$ in x^* (which corresponds to integrating in the physical variable x from L_b to the maximum actual height, h) and from time 0 until when the droplet's velocity is zero results in (after applying some trigonometric identities):

$$\Delta h^* = \frac{\log(C_d^* + 1)}{2C_d^*}. \quad (8)$$

Rewriting this in terms of the height efficiency, $\eta_h \equiv h/H$ and defining $L^* \equiv L_b/d$ and $\text{Fr}_d \equiv V_0^2/(gd)$ results in the following expression:

$$\eta_h = \frac{2L^*}{\text{Fr}_d} + \left(1 - \frac{2L^*}{\text{Fr}_d} \right) \frac{\log(C_d^* + 1)}{C_d^*}. \quad (9)$$

After defining a non-dimensionalized droplet diameter $D^* \equiv D/d$, C_d^* can be written as

$$C_d^* = \frac{3 \rho_g C_d}{4 \rho_l D^*} (\text{Fr}_d - 2L^*). \quad (10)$$

The reader should recognize the explicit dependence of C_d^* on Fr_d . The reduced drag coefficient C_d^* can not physically be less than zero, suggesting a critical Froude number exists where $\text{Fr}_{d,\text{crit}} = 2L^*$. Note that when $C_d^* = 0$, η_h is unity by equation 9.

Existing correlations for the breakup distance L_b and representative droplet diameters D can be used with equation 9 to estimate the jet height efficiency.

Comparison of theory with experiments of Arato, Crow, and Miller [9]. Arato, Crow, and Miller [9] conducted vertical fountain height experiments with a variety of nozzles. Their main nozzle had a diameter of 25.65 mm. Unfortunately, they provided no measurements of the breakup characteristics of their nozzles. Consequently, we used an existing experimental correlation for the breakup length for fully developed turbulent flow in the appropriate Weber number range [23]¹:

$$L^* = 7.40 \text{We}_{ld}^{0.34}. \quad (11)$$

¹Though the correlation is valid only for $1.0 \cdot 10^2 < \text{We}_{ld} < 1.1 \cdot 10^6$, we use it down to a Weber number of zero for simplicity.

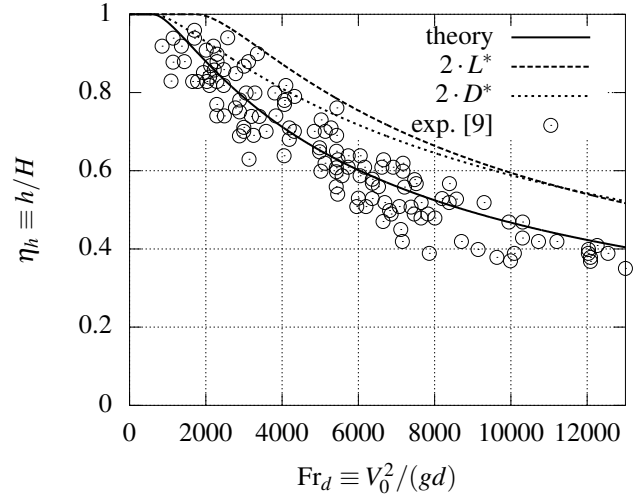


FIGURE 1. Comparison between theoretical jet height efficiency as predicted by equation 9 and as measured by Arato, Crow, and Miller [9]. Also included is a sensitivity analysis of equation 9 to the breakup distance and droplet diameter.

As a distribution of droplet sizes is present in the spray, it is necessary to pick an appropriate representative droplet size. Our interest in this work is the maximum extent of the trajectory, as this often is the only experimental quantity available. As previous research has suggested, smaller Froude numbers increase this maximum extent. Thus, the largest droplets are launched farthest. The representative droplet size was chosen to be 0.75 times the nozzle diameter (i.e., $D^* = 0.75$) to match the experimental data reasonably well. This value is reasonable given that the largest structures far from the nozzle exit are roughly that size [24]. The fit becomes poorer as the nozzle Froude number increases. The poor fit at high Froude numbers may be due to the largest droplet size decreasing as the Weber number increases, the droplet shape changing farther from spherical as the Weber number increases (increasing the drag coefficient), or air entrainment. However, we have not tested these hypotheses.

The density of air was taken to be $\rho_g = 1.2 \text{kg/m}^3$, the density of water was taken to be $\rho_l = 1000 \text{kg/m}^3$, the drag coefficient for the droplets was taken to be that of a sphere at high Reynolds number, $C_d = 0.47$.

The height efficiency is plotted in figure 1. The comparison is excellent, suggesting that even a model as simple as that just developed captures most of the relevant physics.

Note that the Bond number ($\text{Bo}_{ld} \equiv \rho_l g d^2 / \sigma = \text{We}_{ld} / \text{Fr}_d$) for each experimental point was not necessarily the same as that for the model line. This was because each point corresponds to a particular nozzle diameter which was not specified in the original plot or text. We assumed all these diameters were 25.65 mm. The Bond number variation likely contributed to the spread of the data,

but it does not seem to have been large enough to cause additional problems.

Observations. From equation 9, some general observations can be made. First, increasing the breakup distance (through L^*) always increases the jet height efficiency. Thus, nozzle designs that explicitly choose to increase the breakup distance will improve the jet height efficiency. As will be shown in the next section, the same result also applies in the more general (flat-fired) trajectory case.

The second observation is that larger droplets (through D^*) increase the jet height efficiency. This is consistent with past tests which have indicated that fine mist sprays have poor range [25].

The sensitivities of the vertical height to the breakup distance, L^* , and the representative droplet diameter, D^* , are relevant. As can be seen in figure 1, doubling the breakup distance has a similar effect to doubling the representative droplet size. Increasing the breakup distance from nozzles used in practice by a factor of 2 may be possible given that merely changing the length of the nozzle can increase the breakup distance by about a factor of about 10 [10]. However, increasing the largest droplet size is not likely given that all droplets tend to be smaller than the nozzle diameter in the range of Weber numbers seen in this case [4].

As previously noted, a critical Froude number exists, such that the jet height efficiency will be 1 below this Froude number. Equation 9 suggests that $\eta_h = 1$ when $C_d^* = 0$. Solving for the critical Froude number from the definition of C_d^* returns

$$Fr_{d,crit} = 2L^*(We_{ld,crit}), \quad (12)$$

where L^* is written as a function of the Weber number corresponding to the critical Froude number for clarity. L^* in this expression is a function of $We_{ld,crit} \equiv Bo_{ld}Fr_{d,crit}$. Then equation 12 can be rearranged to state

$$Fr_{d,crit} = 2L^*(Bo_{ld}Fr_{d,crit}). \quad (13)$$

The critical Froude number is solely a function of the Bond number for a particular nozzle. Equation 13 combined with the correlations used indicate that $Fr_{d,crit}$ is about 600 for the nozzles used by Arato, Crow, and Miller [9]. It is worth highlighting that this argument assumes that L^* is only a function of We_{ld} . Alternative correlations could have different functional dependencies, e.g., including the Reynolds number. Wu and Faeth [23] demonstrate, however, that a large amount of data is well correlated by solely the liquid Weber number.

Also, in principle, the critical Froude number can be found without solving for the entire trajectory with drag. The critical Froude number occurs when the breakup length equals the distance the jet travels. In this case, one could find the critical Froude

number by setting $H = L_b$ and rearranging the result into a Froude number.

3 HORIZONTAL RANGE ANALYSIS

The “flat-fire” trajectory (here named “flat-fired” to distinguish it from deflagrations) is an approximation to the ballistic trajectory of a projectile for shallow or small firing angles above horizontal (θ_0). This approach can lead to an implicit equation for the range. In this work, the flat-fired approximation is applied to the water jet case to gain an understanding of the factors which control its trajectory. McCoy [26] and Carlucci [27] detail this approximation and its historical use. The flat-fired approximation will be compared to the numerical evaluation of the trajectory to determine the limits of its validity.

The general solution procedure loosely follows that used for the vertical fountain case. The same assumptions as before are made (the droplets do not interact or change diameter and air entrainment is neglected). The first step is to solve the dragless part of the trajectory. The governing equations and initial conditions are

$$\begin{aligned} \ddot{x} &= 0, & \ddot{y} &= -g \\ x(0) &= 0, & y(0) &= h_0 \\ \dot{x}(0) &= V_0 \cos \theta_0, & \dot{y}(0) &= V_0 \sin \theta_0. \end{aligned} \quad (14)$$

Note that x is the horizontal direction and y is vertical. The solution of these equations is

$$x = V_0 \cos \theta_0 t, \quad y = V_0 \sin \theta_0 t - \frac{1}{2}gt^2 + h_0. \quad (15)$$

Existing correlations for breakup distance neglect the effect of gravity changing the trajectory of the jet. It seems reasonable to assume that in the case where the trajectory is bent (e.g., from gravity), the jet breaks up when its arc-length equals the breakup length. We are not aware of research investigating the effect of gravity and launch angle on breakup length of a jet, so this assumption is necessary. At worst, this assumption is accurate for trajectories with small deviations from a straight line. Unfortunately, for the dragless trajectory, the arc-length expression is too messy to be usable. Consequently, the approximation $V_0 t_b = L_b$ will be used to calculate a breakup time, t_b , which will be used to find the x and y locations of the breakup, x_b and y_b . This approximation is exact for a straight line trajectory, and consequently it becomes more accurate as gravity becomes less important, i.e., as the Froude number increases. Applying this approximation

results in

$$x_b = x(t_b) = V_0 \cos \theta_0 \frac{L_b}{V_0} = L_b \cos \theta_0, \quad (16)$$

$$\begin{aligned} y_b = y(t_b) &= V_0 \sin \theta_0 \frac{L_b}{V_0} - \frac{1}{2} g \left(\frac{L_b}{V_0} \right)^2 + h_0 \\ &= L_b \sin \theta_0 - \frac{gL_b^2}{2V_0^2} + h_0. \end{aligned} \quad (17)$$

The corresponding velocities at breakup are

$$\dot{x}_b = u_b = \dot{x}(t_b) = V_0 \cos \theta_0, \quad (18)$$

$$\dot{y}_b = v_b = \dot{y}(t_b) = V_0 \sin \theta_0 - \frac{gL_b}{V_0}. \quad (19)$$

To define the range efficiency ($\eta_R \equiv R/R_{\max, h_0=0}$), the maximum range a jet can obtain without drag must first be found. If the starting height (h_0) is zero, one can show that the maximum range a dragless particle can obtain occurs at a firing angle of $\pi/4$ radians and is $R_{\max, h_0=0} = V_0^2/g$. Note that unlike η_h , η_R is not bounded by 1 for nonzero starting heights. Elevated starting heights increase range over than the reference case where there is no starting height. Developing an explicit equation for range efficiency that takes starting height into account is not possible, as the optimal firing angle is a strong function of Fr_{h_0} . The maximum range must be found by solving an implicit equation. Also note that as η_R is not bounded by 1, it is not possible to make comparisons between different firing angles in terms of efficiency with η_R ; one must convert to a formulation where R_{\max} takes into account the starting height. As the firing angle is basically fixed in applications, this is not a major concern.

The droplet part of the trajectory is governed by the equation

$$m_D \frac{d^2 \vec{x}}{dt^2} = -m_D \vec{g} - \frac{1}{2} \rho_g C_d A_D \left| \frac{d\vec{x}}{dt} \right| \frac{d\vec{x}}{dt}. \quad (20)$$

This equation is non-dimensionalized with $\tau \equiv t/(V_0/g)$ and $\vec{x}^* \equiv \vec{x}/(V_0^2/g)$ to return

$$\frac{d^2 \vec{x}^*}{d\tau^2} = -\hat{j} - C_d^* \left| \frac{d\vec{x}^*}{d\tau} \right| \frac{d\vec{x}^*}{d\tau} \quad (21)$$

where

$$C_d^* \equiv \frac{3}{4} \frac{\rho_g}{\rho_l} C_d \frac{V_0^2}{gD} = \frac{3}{4} \frac{\rho_g}{\rho_l} C_d \frac{Fr_d}{D^*}, \quad (22)$$

which is similar to the definition used in the vertical case, except that the velocity here is V_0 . This selection was found to greatly simplify the result when compared against the result from selecting the breakup velocity. The breakup velocity had been used in the vertical fountain case.

The flat-fired approximation suggests that for small firing angles (θ_0), the droplet velocity approximately equals \dot{x} because \dot{y} is small. Mathematically, this states

$$\left| \frac{d\vec{x}^*}{d\tau} \right| \approx \frac{dx^*}{d\tau}. \quad (23)$$

After defining

$$u^* \equiv \frac{dx^*}{d\tau} \quad \text{and} \quad v^* \equiv \frac{dy^*}{d\tau}, \quad (24)$$

the resulting system of ODEs to solve is

$$\frac{du^*}{d\tau} = -C_d^* (u^*)^2, \quad (25)$$

$$\frac{dv^*}{d\tau} = -1 - C_d^* u^* v^*. \quad (26)$$

Overprediction of η_R is expected with this approximation, with the overprediction being worse at larger angles. This is because the effective drag force is lower in a flat-fired trajectory than a real one.

The non-dimensionalized initial conditions for the breakup stage are

$$x_b^* = x^*(0) = \frac{gL_b}{V_0^2} \cos \theta_0 = \frac{L^*}{Fr_d} \cos \theta_0, \quad (27)$$

$$y_b^* = y^*(0) = \frac{L^*}{Fr_d} \sin \theta_0 - \frac{1}{2} \left(\frac{L^*}{Fr_d} \right)^2 + \frac{1}{Fr_{h_0}}, \quad (28)$$

$$u_b^* = \cos \theta_0, \quad (29)$$

$$v_b^* = \sin \theta_0 - \frac{L^*}{Fr_d}. \quad (30)$$

After applying the initial conditions, the solutions of equa-

tions 25 and 26 are

$$u^* = \frac{u_b^*}{u_b^* C_d^* \tau + 1}, \quad (31)$$

$$x^* = \frac{\log(u_b^* C_d^* \tau + 1)}{C_d^*} + x_b^*, \quad (32)$$

$$v^* = -\left(\frac{u_b^* C_d^* \tau + 1}{2u_b^* C_d^*}\right) + \frac{1}{u_b^* C_d^* \tau + 1} \left(v_b^* + \frac{1}{2u_b^* C_d^*}\right), \quad (33)$$

$$y^* = -\left(\frac{u_b^* C_d^* \tau + 1}{2u_b^* C_d^*}\right)^2 + \left(\frac{v_b^*}{u_b^* C_d^*} + \frac{1}{2(u_b^* C_d^*)^2}\right) \log(u_b^* C_d^* \tau + 1) + \frac{1}{4(u_b^* C_d^*)^2} + y_b^*. \quad (34)$$

Note that from the solution for x^*

$$C_d^* (x^* - x_b^*) = \log(u_b^* C_d^* \tau + 1). \quad (35)$$

The time when the droplets impact the ground is defined as τ_R . Note that $x^*(\tau_R) = \eta_R$ because $x^* \equiv xg/V_0^2$ and thus if $x = R$ at $\tau = \tau_R$ then $x^*(\tau_R) = Rg/V_0^2 \equiv \eta_R$.

To find τ_R , equation 34 can be used. By definition, the droplets impact the ground at time τ_R , and thus the dimensionless height above the ground (y^*) is zero:

$$y^*(\tau_R) = 0 = -\left(\frac{u_b^* C_d^* \tau_R + 1}{2u_b^* C_d^*}\right)^2 + \left(\frac{v_b^*}{u_b^* C_d^*} + \frac{1}{2(u_b^* C_d^*)^2}\right) \underbrace{\log(u_b^* C_d^* \tau_R + 1)}_{\text{equation 35}} + \frac{1}{4(u_b^* C_d^*)^2} + y_b^*. \quad (36)$$

Equation 35 can be used to simplify one of these terms. After substituting in that term and rearranging, the result is

$$u_b^* C_d^* \tau_R + 1 = \left[(2C_d^* v_b^* u_b^* + 1) 2C_d^* (\eta_R - x_b^*) + 1 + y_b (2u_b^* C_d^*)^2 \right]^{1/2}, \quad (37)$$

which can be substituted back into equation 35 to find an implicit algebraic equation for η_R :

$$2C_d^* (\eta_R - x_b^*) = \log \left[(2C_d^* v_b^* u_b^* + 1) 2C_d^* (\eta_R - x_b^*) + 1 + y_b (2C_d^* u_b^*)^2 \right]. \quad (38)$$

Substituting in the values of the initial conditions returns the result seen in equation 39. This is the equation for η_R provided models for L^* and D^* are used and that all of the constants are available.

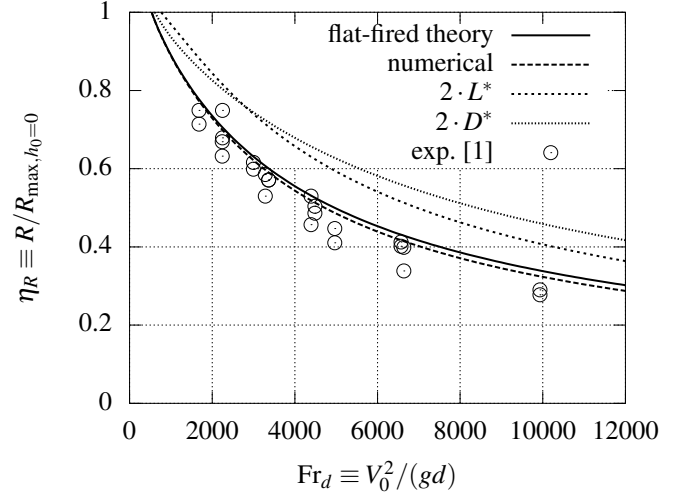


FIGURE 2. Comparison between flat-fired theory (equation 39) and experimental data from Theobald [1] for $\theta_0 = 35^\circ$. Note that the numerical solution is the one directly below the solid black line. Also plotted is sensitivity analysis of η_R to the breakup distance and droplet diameter for the same firing angle.

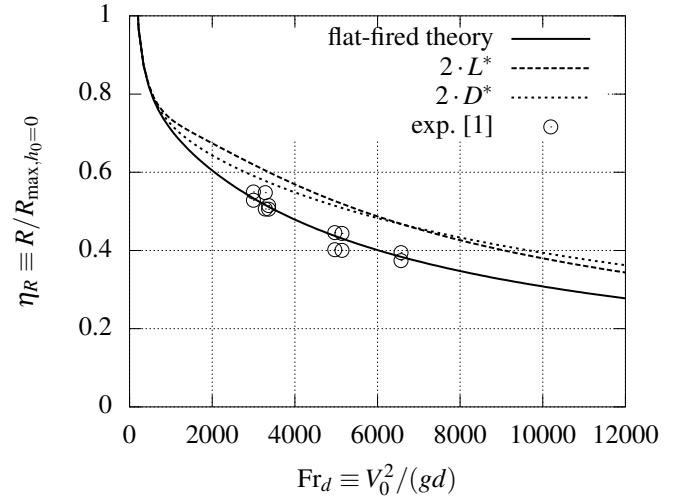


FIGURE 3. Comparison between flat-fired theory (equation 39) and experimental data from Theobald [1] for $\theta_0 = 20^\circ$. The numerical solution is not plotted, as it was essentially coincident with the black line. Also plotted is sensitivity analysis of η_R to the breakup distance and droplet diameter for the same firing angle.

$$\frac{3 \rho_g C_d Fr_d}{2 \rho_l D^*} \left(\eta_R - \frac{L^*}{Fr_d} \cos \theta_0 \right) = \log \left[\left(\frac{3 \rho_g C_d Fr_d}{2 \rho_l D^*} \left(\sin \theta_0 - \frac{L^*}{Fr_d} \right) \cos \theta_0 + 1 \right) \frac{3 \rho_g C_d Fr_d}{2 \rho_l D^*} \left(\eta_R - \frac{L^*}{Fr_d} \cos \theta_0 \right) + 1 + \left(\frac{L^*}{Fr_d} \sin \theta_0 - \frac{1}{2} \left(\frac{L^*}{Fr_d} \right)^2 + \frac{1}{Fr_{h_0}} \right) \left(\frac{3 \rho_g C_d Fr_d}{2 \rho_l D^*} \cos \theta_0 \right)^2 \right]. \quad (39)$$

Comparison with experiments of Theobald [1]. Equation 39 was compared against experiments done by Theobald [1] in figures 2 and 3. These experiments are presently the only trajectory tests available in the literature conducted indoors, which eliminated the influence of wind. This is necessary as the model does not account for wind and intermittent wind can be difficult to account for.

The fit between Theobald's data and the model is reasonable. The same breakup length correlation (equation 11) and representative dimensionless droplet size ($D^* = 0.75$) used in the vertical height case are used here.

Also plotted is the numerical solution to the full trajectory equations without approximation (equation 21), showing excellent fit between the numerical and approximate solution despite the fact that 35° is not a small angle. The small error demonstrates the accuracy of the flat-fired approximation up through relatively large angles.

As in the vertical height case, the Bond number (Bo_{1d}) for each experimental point was not necessarily the same as that for the model. Again, the Bond number does not appear to vary adequately to cause a poor fit.

Observations. As can be inferred from figures 2 and 3, the sensitivity of the flat-fired solution to increases in the breakup length and representative droplet size are consistent with those seen in the vertical height case. At larger firing angles, the range increases more greatly as the droplet size increases.

Consistent with the vertical height case, it is unlikely that the size of the largest droplets in the spray could increase to improve the range. However, this does not indicate that droplet size is unimportant for range. In the trajectory case, the distribution of water on the surface is important. The droplet size distribution will strongly influence the distribution of water on the surface. Thus, increasing the size of the smallest droplets would prove advantageous where a more compact distribution is desired, as is the case in hose stream fire protection. In contrast, increasing the spread of the droplet size distribution would prove advantageous in jet sprinkler irrigation, as a uniform distribution of water on the ground is desired.

The critical Froude number of the trajectory is difficult to find analytically. A critical Froude number could be found from this analysis, however, its accuracy would be suspect because of

the estimate of the arc-length used. This estimate is inaccurate when the coherent portion of the jet is not almost a straight line, which is true for low Froude numbers, where the critical Froude number is. The easier approach mentioned in the vertical jet case of setting the breakup length equal to the distance the jet travels (the arc-length) is not feasible analytically due to the complexity of the arc-length formula. Also complicating matters is the range non-dimensionalization used. The critical Froude number can be found numerically in this model, if it is desired.

4 CONCLUSIONS

1. Assuming breakup takes place instantaneously, the trajectory of a water jet can be decomposed into components before and after breakup.
2. The trajectory before breakup is well described by the trajectory of a dragless particle, in accordance with potential flow theory and prior experimental observations.
3. The trajectory after breakup is well described by the trajectory of a spherical particle experiencing quadratic drag, as is commonly done for sprays.
4. Increasing breakup length increases both the maximum height of a vertical fountain as well as the maximum range of a nominally horizontally fired water jet.
5. The maximum height and maximum range also increase with the maximum droplet size. However, this size is already nearly as large as it could be, so increasing maximum droplet size is not a viable way to improve range.
6. Increasing the nozzle Froude number strongly reduces the range.
7. Below a certain Froude number, termed the critical Froude number, no breakup occurs and the jet trajectory is that of a dragless particle.

References

- [1] Theobald, C., 1981. "The effect of nozzle design on the stability and performance of turbulent water jets". *Fire Safety Journal*, **4**(1), Aug., pp. 1–13.
- [2] Lebedev, B. M., 1977. *Dozhdeval'nye mashiny (Irrigation systems)*, second ed. Mashinostroenie, Moscow.

- [3] Hickey, H. E., 1980. *Hydraulics for fire protection*. National Fire Protection Association, Boston, Mass.
- [4] Lin, S. P., and Reitz, R. D., 1998. “Drop and Spray Formation from a Liquid Jet”. *Annual Review of Fluid Mechanics*, **30**(1), pp. 85–105.
- [5] Birouk, M., and Lekic, N., 2009. “Liquid jet breakup in quiescent atmosphere: a review”. *Atomization and Sprays*, **19**(6), pp. 501–528.
- [6] Rouse, H., Howe, J. W., and Metzler, D. E., 1952. “Experimental Investigation of Fire Monitors and Nozzles”. *Transactions of the American Society of Civil Engineers*, **117**(1), Jan., pp. 1147–1175.
- [7] Hoyt, J. W., and Taylor, J. J., 1977. “Turbulence structure in a water jet discharging in air”. *Physics of Fluids*, **20**(10), p. S253.
- [8] Freeman, J. R., 1889. “Experiments Relating to Hydraulics of Fire Streams”. *Transactions of the American Society of Civil Engineers*, **XXI**(2), July, pp. 303–461.
- [9] Arato, E. G., Crow, D. A., and Miller, D. S., 1970. Investigations of a high performance water nozzle. Tech. Rep. 1058, British Hydromechanics Research Association, June.
- [10] Arai, M., Shimizu, M., and Hiroyasu, H., 1985. “Break-up length and spray angle of high speed jet”. In Proceedings of ICLASS, pp. IB/4/1–IB/4/10.
- [11] Irvine, D. A., and Falvey, H. T., 1987. “Behaviour of turbulent water jets in the atmosphere and in plunge pools”. *Proceedings of the Institution of Civil Engineers*, **83**(1), Jan., pp. 295–314.
- [12] Wahl, T., Frizell, K., and Cohen, E., 2008. “Computing the Trajectory of Free Jets”. *Journal of Hydraulic Engineering*, **134**(2), pp. 256–260.
- [13] Bilanski, W. K., and Kidder, E. H., 1958. “Factors that affect the distribution of water from a medium-pressure rotary irrigation sprinkler”. *Transactions of the ASAE*, **1**(1), pp. 19–28.
- [14] Szalay, M., 1963. “Az esőztető szórófejek vízszugárballisztikája (Water jet ballistics of sprinkler nozzles)”. *Hidrológiai közlöny*, **4**, pp. 323–327.
- [15] Hatton, A. P., and Osborne, M. J., 1979. “The trajectories of large fire fighting jets”. *International Journal of Heat and Fluid Flow*, **1**(1), Mar., pp. 37–41.
- [16] Hatton, A. P., Leech, C. M., and Osborne, M. J., 1985. “Computer simulation of the trajectories of large water jets”. *International Journal of Heat and Fluid Flow*, **6**(2), June, pp. 137–141.
- [17] Murzabaeb, M. T., and Yarin, A. L., 1985. “Dynamics of sprinkler jets”. *Fluid Dynamics*, **20**(5), Sept., pp. 715–722.
- [18] Isaev, A. P., 1966. “Optimal’nyye rezhimy raboty dal’nostruynykh dozhdeval’nykh mashin (Optimal operating conditions of long-range sprinklers)”. *Mekhanizatsiya i elektrifikatsiya sotsialisticheskogo sel’skogo khozyaystva*, **24**(9), pp. 4–9.
- [19] Tuck, E. O., 1976. “The shape of free jets of water under gravity”. *Journal of Fluid Mechanics*, **76**(04), pp. 625–640.
- [20] Oehler, T., 1958. Characteristics, operational conditions and limits of the performance of rotary rainers / 1. Nozzle shape, jet formation and rate of nozzle discharge. Translation 41, National Institute of Agricultural Engineering, Silsoe, Bedfordshire. English translation of ref. [21].
- [21] Oehler, T., 1957. “Merkmale, Bedingung und Grenzen der Leistungsfähigkeit von Drehstrahlregnern / I. Düsenform, Strahlbildung und Düsenleistung”. *Landtechnische Forschung*, **7**(5), pp. 121–126.
- [22] Kawakami, K., 1971. “Study on the Computation of Horizontal Distance of Jet Issued from Nozzle”. *Proceedings of the Japan Society of Civil Engineers*, **1971**(191), pp. 83–89.
- [23] Wu, P.-K., and Faeth, G. M., 1995. “Onset and end of drop formation along the surface of turbulent liquid jets in still gases”. *Physics of Fluids (1994-present)*, **7**(11), Nov., pp. 2915–2917.
- [24] Hoyt, J. W., and Taylor, J. J., 1977. “Waves on water jets”. *Journal of Fluid Mechanics*, **83**(1), pp. 119–127.
- [25] Grant, G., Brenton, J., and Drysdale, D., 2000. “Fire suppression by water sprays”. *Progress in Energy and Combustion Science*, **26**(2), Apr., pp. 79–130.
- [26] McCoy, R. L., 1999. *Modern Exterior Ballistics: The Launch and Flight Dynamics of Symmetric Projectiles*. Schiffer Publishing, Ltd.
- [27] Carlucci, D. E., 2008. *Ballistics: Theory and Design of Guns and Ammunition*. CRC Press.